

Nanolayer Laser Absorber for Femtoliter Chemistry in Polymer Reactors

Junfang Zhang,* Yuxin Liu, Sebastian Ronneberger, Nadezda V. Tarakina, Nabyl Merbouh, and Felix F. Loeffler*

Laser-induced forward transfer (LIFT) has the potential to be an alternative approach to atomic force microscopy based scanning probe lithography techniques, which have limitations in high-speed and large-scale patterning. However, traditional donor slides limit the resolution and chemical flexibility of LIFT. Here, a hematite nanolayer absorber for donor slides to achieve high-resolution transfers down to sub-femtoliters is proposed. Being wettable by both aqueous and organic solvents, this new donor significantly increases the chemical scope for the LIFT process. For parallel amino acid coupling reactions, the patterning resolution can now be increased more than five times ($>111\,000$ spots cm^{-2} for hematite donor vs $20\,000$ spots cm^{-2} for standard polyimide donor) with even faster scanning (2 vs 6 ms per spot). Due to the increased chemical flexibility, other types of reactions inside ultrasmall polymer reactors: copper (I) catalyzed click chemistry and laser-driven oxidation of a tetrahydroisoquinoline derivative, suggesting the potential of LIFT for both deposition of chemicals, and laser-driven photochemical synthesis in femtoliters within milliseconds can be explored. Since the hematite shows no damage after typical laser transfer, donors can be regenerated by heat treatment. These findings will transform the LIFT process into an automatable, precise, and highly efficient technology for high-throughput femtoliter chemistry.

1. Introduction

Chemical reactions in ultrasmall volumes, for example femtoliters, are showing increasing importance,^[1] since they exhibit a new pathway for the synthesis of nanoparticle libraries,^[2] and drastically improve the throughput of microarrays^[3] and combinatorial screening.^[4] To perform reactions at such levels, it is critical to deliver reagents precisely at specific positions on a surface and control the dispersity of these reactors.^[5] Microfluidic lithography (ML), based on atomic force microscopy (AFM), was shown to be an attractive route for the miniaturization of reactions.^[6] However, many of those approaches have been proven impractical for large-scale patterning or device applications,^[7] with limited scanning speed per cantilever.^[8] As a more flexible direct-writing technology,^[9] laser-induced forward transfer (LIFT) has the potential to be an alternative approach for femtoliter chemistry. In LIFT, materials, coated as a thin layer on a donor substrate, are transferred onto a desired

acceptor by a focused laser. In contrast to standard ML technologies, the scan speed of LIFT can be three orders of magnitude faster ($50\ \mu\text{m s}^{-1}$ ^[10] vs $200\ \text{mm s}^{-1}$) and still be compatible with large-scale patterning. Donor slides, as an essential part of LIFT, highly influence the transfer resolution. Typical donors for LIFT are metal-coated slides, which are usually paired with destructive pulsed lasers.^[11] They are mainly suitable for the transfer of robust materials instead of biomolecules or chemicals, due to overheating and/or metal poisoning.


A recent variant of LIFT exploits low-cost diode lasers to transfer polymer spots (polyLIFT), which incorporate chemical building blocks.^[12] Since the glass transition temperatures of polymers are typically much lower than the melting or boiling temperatures of metals, polyLIFT is compatible with polyimide donors under less intensive continuous wave laser irradiation. The polymer functions as a protective matrix for the chemicals during LIFT, which enables the transfer of fragile chemicals^[12] and nanomaterials.^[13] The mild transfer conditions^[14] and the control over the reaction in polymer reactors, which can be switched on by melting the polymer in an oven,^[15] allow for a new approach for chemical reactions in the femtoliter range. Furthermore, these polymer reactors enable easy control of the spot size for combinatorial chemistry, in comparison

J. Zhang, Y. Liu, S. Ronneberger, N. V. Tarakina, F. F. Loeffler
Max-Planck-Institute of Colloids and Interfaces
Am Muehlenberg 1, 14476 Potsdam, Germany
E-mail: Junfang.Zhang@mpikg.mpg.de; felix.loeffler@mpikg.mpg.de

J. Zhang, Y. Liu
Institute of Chemistry and Biochemistry
Free University of Berlin
14195 Berlin, Germany

S. Ronneberger
Institute of Physics and Astronomy
University of Potsdam
Campus Golm, Karl-Liebknecht-Straße 24/25
14476 Potsdam, Germany

N. Merbouh
Department of Chemistry
Simon Fraser University
8888 University Drive, Burnaby, BC V5A 1S6, Canada

 The ORCID identification number(s) for the author(s) of this article can be found under <https://doi.org/10.1002/adma.202108493>.

© 2022 The Authors. Advanced Materials published by Wiley-VCH GmbH. This is an open access article under the terms of the Creative Commons Attribution License, which permits use, distribution and reproduction in any medium, provided the original work is properly cited.

DOI: 10.1002/adma.202108493

with liquid droplets, which have problems of evaporation and diffusion. Nevertheless, the polyimide donor suffers from deformation and degradation (i.e., carbonization) during laser irradiation,^[16] which limits its reusability and the resolution of polyLIFT.

Here, we propose a robust hematite (α -Fe₂O₃) nanolayer as the absorber for high-resolution polyLIFT (polyLIFT_h) to achieve transfers down to the sub-femtoliter regime, which is even smaller than for ML technologies (0.5 ± 0.2 vs 42.7 ± 2.3 fL^[5]). The hematite nanolayer is obtained by a facile annealing process and shows no contamination with iron on the acceptor surface. Since this nanolayer is wettable by both aqueous and organic solvents, the new donor significantly increases the scope of polymers for the polyLIFT_h process. For parallel amino acid coupling reactions, our hematite donor enables five times higher patterning resolution ($20\,000$ vs $>111\,000$ spots cm⁻²) with more efficient scanning (2 vs 6 ms per spot) comparing with the standard polyimide donor. Due to the large polymer scope, we could explore the possibility to run other types of reactions inside ultrasmall polymer reactors: copper (I) catalyzed click chemistry and laser-driven in situ oxidation of a tetrahydroisoquinoline derivative, suggesting the potential of LIFT for both chemical deposition and in situ synthesis in sub-femtoliters. Since the hematite shows no damage after a typical transfer, the polymer layer on the donor slides can be reused by simple recovery with a heating step. These findings transform the polyLIFT_h process into an automatable, precise, and highly efficient technology for high-throughput femtoliter chemistry.

2. Results and Discussion

2.1. Synthesis and Characterization of Nanolayer Absorber

For the polyLIFT process, desired materials or chemicals are dissolved together with a polymer matrix in a solvent and coated onto donor slides. The donor absorber layer is heated by laser irradiation, resulting in the melting and transfer of the polymer matrix together with the material onto the surface of an acceptor slide (Figure S1, Supporting Information). Compared to our previous work, polyLIFT_h relies on the here introduced nanolayer absorber. We added iron (III) nitrate as a metal precursor into a mixture of poly(vinyl alcohol) (PVA) and poly(ethylene glycol) (PEG) (Figure 1a). This solution was spin-coated onto a glass substrate and the film was annealed in an air oven at 500 °C for 3 h. The morphology of the obtained layer (Figure S2, Supporting Information) shows homogeneously distributed structure with long-distance order. The X-ray diffraction spectrum (Figure 1b) and XPS spectrum (Figure S3, Supporting Information) reveal that the obtained film is polycrystalline hematite (α -Fe₂O₃).^[17] Based on the Scherrer equation, the grains should be subspheroidal with an average grain size of 38.2 ± 3.1 nm. Elemental analysis shows no residual carbon (Figure S4, Supporting Information), suggesting the complete decomposition of the polymer and the metal precursors. Moreover, hematite has a thermal stability of above 1000 °C (Figure S4, Supporting Information), providing the possibility for a wide range of LIFT applications. Transmission electron microscopy (TEM) (Figure 1c) further confirm the

well-crystallized structure of the film. Analysis of selected-area electron diffraction (SAED) patterns and fast Fourier transforms obtained from high-resolution images indicates that Fe₂O₃ crystallizes in a hexagonal lattice, with unit cell parameters: $a = 5.02(19)$ Å, $c = 13.5(7)$ Å. The hematite layer has a thickness of around 81 nm (Figure S5, Supporting Information), which is much thinner than the typical polyimide film used for polyLIFT (≈ 25 μm polyimide with siloxane-based adhesive, ≈ 54 μm in total). Thus, the hematite donor should have a drastically reduced heat capacity, theoretically enabling transfer resolutions as small as the laser spot.

Next, we characterized the optical properties of hematite layers. In contrast to polyimide, our hematite film shows a significant redshift of absorption in the UV–vis spectrum (Figure 1d). By plotting $(\alpha h\nu)^2$ as a function of $h\nu$ (Figure S6, Supporting Information), the bandgaps of the hematite and polyimide were calculated to be 2.07 eV (600 nm) and 2.56 eV (485 nm) respectively, suggesting that hematite has an extended absorption. The behavior of the donor slides under laser irradiation of LIFT setup (488 nm, Figure S7, Supporting Information) along with increasing input power was measured with an optical sensor (Figure S8, Supporting Information). The absorption efficiency of hematite stabilizes around 90%, while that of polyimide keeps decreasing to $\approx 80\%$. The near-constant absorption efficiency of hematite donors avoids the uncertain factors during practical synthesis, which can further guarantee the reproducibility. Typically for LIFT, the absorber layer is damaged and partially transferred to the acceptor.^[18] For our hematite nanolayer, energy-dispersive X-ray mapping (Figure 1e), and spectrum (Figure S9, Supporting Information) show no iron contamination is present in the elemental distribution map of transferred polystyrene (PS) spots. Using much more sensitive inductively coupled plasma measurements, we observed no significant increase in iron concentration above the background (0.021 mg g⁻¹) for large area polymer transfers (2.4×6.5 cm²) with maximum laser power (129 mW) and down to 30 mm s⁻¹ scan speed. Only for even slower scan speeds that cause visible ablation of the hematite film from the glass substrate, we observed significant amounts of iron (0.243 mg g⁻¹) on the acceptor slides.

2.2. Increased Resolution for Sub-Femtoliter Reactors

PS is one of the model polymer matrices in our standard LIFT process. Following the characterization of the hematite layer, we transferred PS gradients from both polyimide and hematite donors (Figure S10, Supporting Information). We measured the size and thickness of each spot by vertical scanning interferometry to select the optimum parameters for the smallest reproducible spots from each donor: 31 mW laser power, 2 ms per spot, and 64 mW laser power, 6 ms per spot are used for hematite and polyimide donors, respectively (Figure 2a). While the polyimide donor yields spots of typically 120 μm in diameter, the hematite donor shows much smaller spots of about 30 μm in diameter (Figure 2b). Therefore, 30 μm pitch spot arrays (density: $111\,000$ spots cm⁻²) are achievable with hematite donors (Figure S11, Supporting Information). The hematite donors do not only allow for about four times higher printing

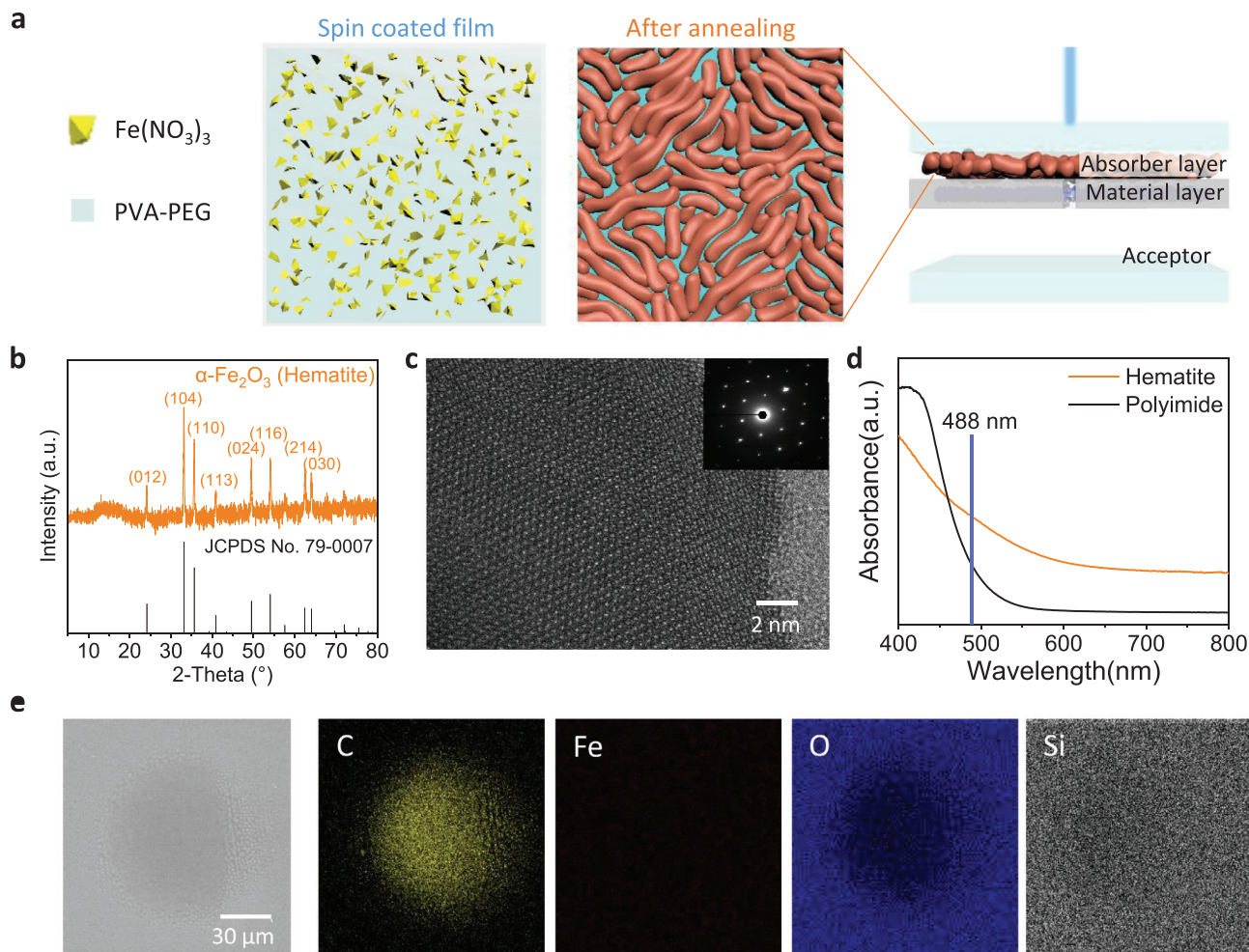


Figure 1. Preparation and characterization of the hematite layer on a glass donor slide. a) Hematite nanofilms are prepared by spin-coating a mixed solution of iron nitrate, PVA, and poly(ethylene glycol), followed by an annealing step. In the polyLIFT_n process, material is transferred from a donor to an acceptor by laser irradiation. b) X-ray diffraction spectrum, c) TEM imaging, and SAED of the hematite nanolayer. d) UV-vis spectrum of the hematite nanolayer and a standard 25 μm-thick polyimide film. e) Energy-dispersive X-ray mapping of a transferred spot on the acceptor slide. No iron contamination is observed.

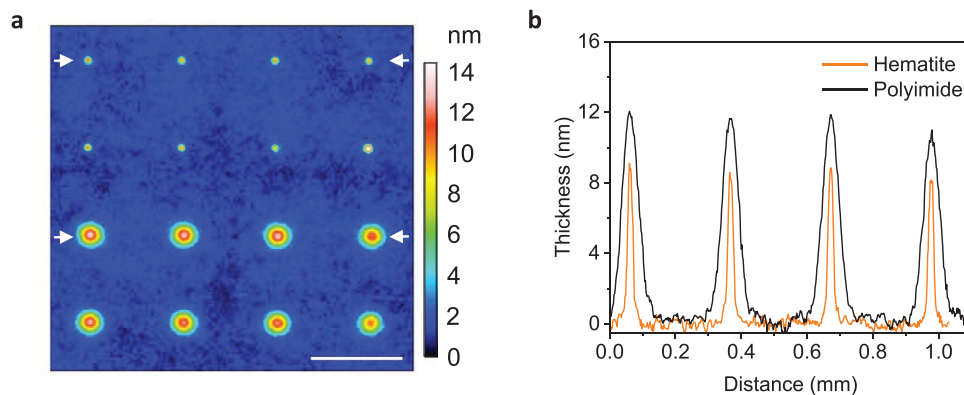


Figure 2. a) Optimized transfer conditions (see Figure S10, Supporting Information) of the smallest observable spots from the hematite donor (top two rows, 31 mW, 2 ms per spot) and polyimide donor (bottom two rows, 64 mW, 6 ms per spot). b) Profiles of the spots in the selected line (marked by white arrows). Scale bar: 300 μm.

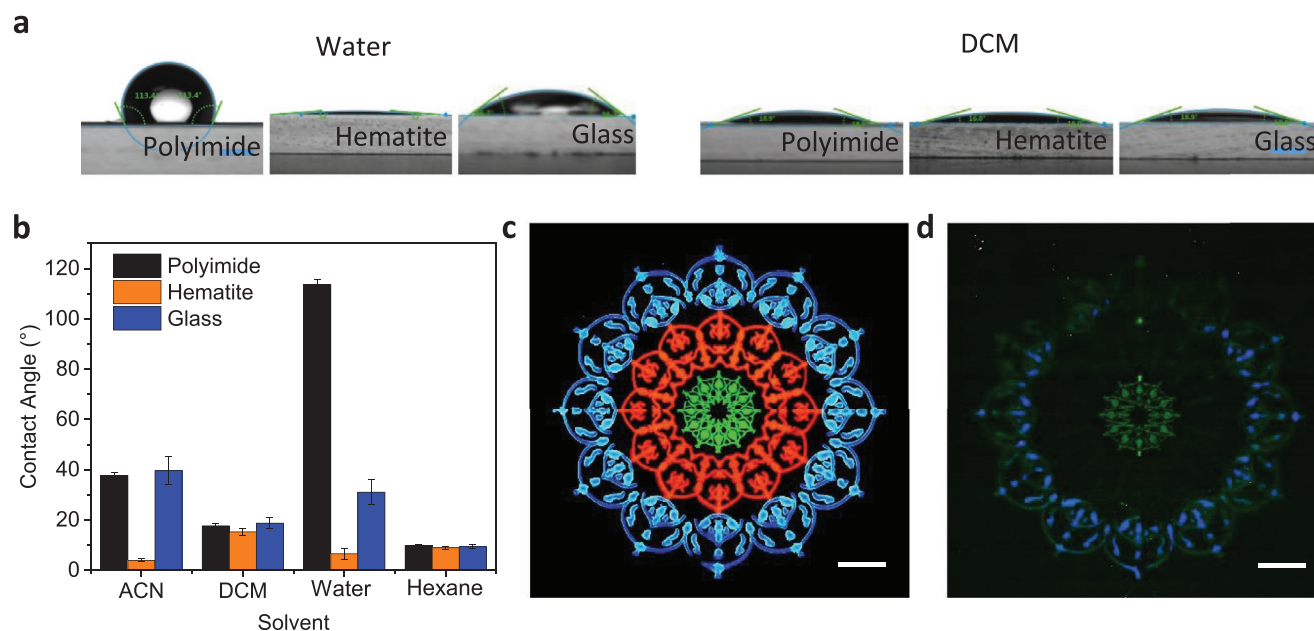


Figure 3. Wettability of hematite donor slides for different solvents. a,b) Contact angles of solvent droplets on different surfaces. c,d) Transferred patterns from hematite donor (c) and polyimide donor (d). Green pattern: polystyrene and Rhodamine B dissolved in DCM; red pattern: PVA and Nile blue dissolved in water; blue pattern: PVP and fluorescein dissolved in water (pattern created by shakeelbaloch—pngtree.com, reproduced with permission). Scale bar: 2 mm.

resolution, but also make the transfer process more time- and energy-efficient (62 vs 384 μ J). To calculate the volume of the spots, we generated 100 spots from both donors using the above-mentioned parameters (Figures S12 and 13, Supporting Information). A threshold detection method was applied. The mean volume of the spots from the polyimide donor is 5.5 ± 4.1 fL, which makes polyLIFT comparable with more complex and expensive microfluidic pen lithography (42.7 ± 2.3 fL^[5]). The new hematite donor reduces the spot volume further to sub-femtoliter range of 0.5 ± 0.2 fL. This indicates the potential of polyLIFT_h as an alternative approach for femtoliter chemistry.

2.3. Expanding the Scope of Polymer Reactors

With standard polyimide donors, transfer of water-soluble polymers, such as PVA, is a big challenge. The main reason for the insufficient transfer is the pronounced hydrophobicity of the polyimide donor (Figure 3a). After being modified with a hematite layer, the contact angle of bare glass dramatically decreases to 3.2° for water, suggesting improved hydrophilicity. Moreover, hematite shows outstanding wettability also for organic solvents, including both polar (acetonitrile) and nonpolar solvents (dichloromethane (DCM) and hexane, Figure 3b). By adding fluorescent dyes into the polymer solutions (fluorescein in poly(vinylpyrrolidone) (PVP), Nile blue in PVA, Rhodamine B in PS), the transferred patterns on the acceptors can be observed by fluorescence scanning (Figure 3c,d). While the PVA and PVP transfer from the polyimide donor shows low quality with incomplete areas, the hematite donor achieves precise and homogenous patterns. This is further supported by thickness measurements of the transferred patterns (Figure S14, Supporting Information). The successful transfer of water-soluble

polymer expands the scope of molecules we can deliver with the polyLIFT_h method and opens up the possibility for many more types of reactions in ultrasmall polymer reactors.

2.4. Femtoliter Chemistry in Polymer Reactors

As a start, we selected the amide bond formation and performed reactions in ultrasmall polymer reactors. This reaction is crucial for the synthesis of biomolecule microarrays. Surface-bound (bio)molecule microarrays play an important role in the efficient identification of therapeutic targets, biomarkers, and vaccine candidates.^[19] To check the possibility of polyLIFT_h for high-resolution peptide synthesis, we transferred an amino acid building block (Fmoc-Gly-OPfp: pentafluorophenyl-activated fluorenylmethoxycarbonyl protected glycine) in the PS matrix with decreasing spot pitch onto an amino-functionalized glass surface (Figure 4a). Liquid chromatography–mass spectrometry analysis shows that Fmoc-Gly-OPfp is still present in its active ester form after laser transfer (Figure S15, Supporting Information). The following coupling step proceeds at 95°C for 10 min. During that, the polymer “melted” which allowed the reaction between the building block and surface-bound amino groups. Then, the protective Fmoc groups are cleaved by piperidine, so that an *N*-hydroxysuccinimide activated dye can be attached to the free amino groups for fluorescence imaging. A clear spot array can be observed down to a pitch of $30\ \mu\text{m}$ (vs $70\ \mu\text{m}$ for the polyimide donor, Figure 4b), which is comparable with scanning probe lithography technologies.^[20] Though fluorescent profiles of spots with $30\ \mu\text{m}$ pitch show similar intensity for polyimide and hematite donor, only the spots from the hematite donor are distinguishable (Figure S16, Supporting Information). Furthermore, we successfully transferred and

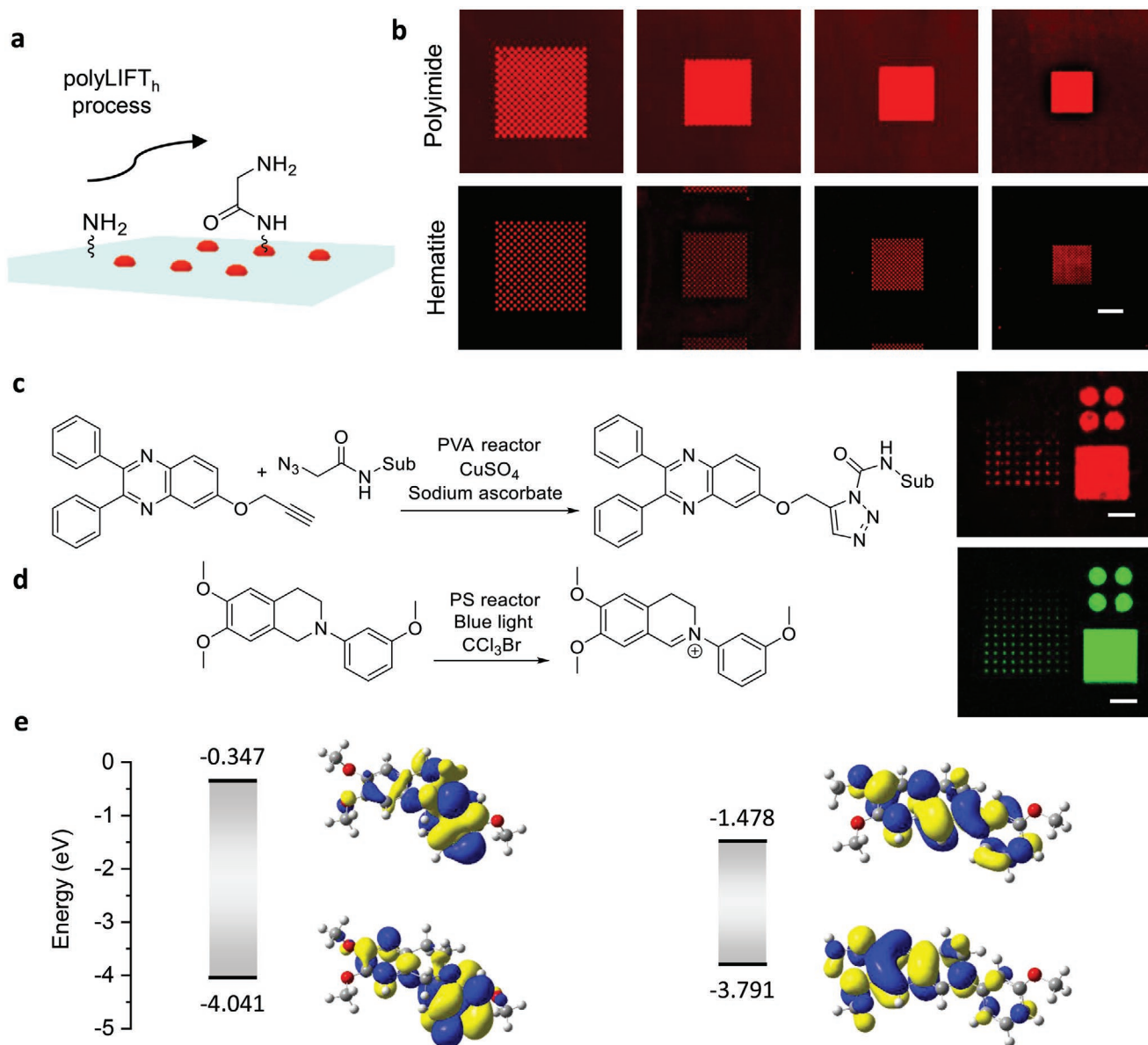


Figure 4. Femtoliter chemistry with polyLIFT_h. a) Transfer of an amino acid building block by polyLIFT_h and subsequent coupling onto an amino-functionalized acceptor slide. b) Amide bond formation in a chess-board pattern (25×25 theoretical spots), achieved for different pitches, from left to right: 70, 50, 40, 30 μm. c) Click chemistry performed in femtoliter PVA reactors. d) In situ oxidation of a tetrahydroisoquinoline derivative by polyLIFT_h. e) Molecular orbital amplitude plots of the substrate and oxidized product. Calculations were performed at B3LYP/6-31G* level. Scale bar: 500 μm.

coupled a second building block, showing the possibility of high-resolution arrays in multistep syntheses (Figure S17, Supporting Information). However, multistep synthesis requires the removal of the acceptor slide from the laser setup for the coupling steps. Thus, the resolution of the synthesis strongly depends on the possibility of precise repositioning of the acceptor slide in the laser setup.

Next, we also performed click chemistry with polyLIFT_h. This process was impossible with standard polyimide donors, since they can only be used with PS matrix. The hematite donor is compatible with many more polymer matrices. Since copper(I)-catalyzed azide-alkyne cycloaddition (CuAAC) requires aqueous conditions, water-soluble PVA was selected as a matrix to

generate suitable reactors (Figure 4c). First, an amino glass surface was functionalized with azidoacetic acid to obtain surface-bound azide groups. An alkyne functionalized dye, 2,3-diphenyl-6-(prop-2-yn-1-yloxy)quinoxaline (i.e., Alk-DQ), was designed and synthesized according to our previous work.^[21] Alk-DQ and the copper catalyst were transferred within PVA by polyLIFT_h, followed by an oven step at 100 °C for 3 h to drive the CuAAC. After washing away the unreacted Alk-DQ, the slide was scanned at 635 nm. To validate the result, which could come from noncovalent interaction between the surface and fluorescent dye, a control experiment was performed, where the surface was not functionalized with the azidoacetic acid. The significantly different fluorescence signals between

click experiment and control experiment (Figure S18, Supporting Information) suggests that the successful CuAAC functionalization was achieved by polyLIFT_h.

Delivery of chemicals and driving the reaction in ultrasmall reactors are essential and challenging for femtoliter chemistry. Here, polyLIFT_h offers a new approach to achieve this goal. Moreover, it shows potential even for in situ laser-driven photooxidation within milliseconds. The 1,2,3,4-tetrahydroisoquinolines (THIQ) core is present in many natural and synthetic products, representing an interesting scaffold for pharmaceutical purposes. The activation of THIQ is a benchmark reaction in cross dehydrogenative coupling research. It is reported that THIQ can be oxidized by bromotrichloromethane (CBrCl₃) under blue light irradiation in 30 min. Since the laser typically has a much higher intensity than normal LED, it may even further speed up photochemical reactions. However, direct exposure under focused laser may be destructive for many chemicals. The polyLIFT_h process solves this problem by letting a small part of the laser irradiation pass through to the chemicals and the protective polymer matrix. A solution of PS, CBrCl₃, and 6,7-dimethoxy-2-(3-methoxyphenyl)-1,2,3,4-tetrahydroisoquinoline (TM-THIQ) was spin-coated on the surface of the hematite donor. This freshly prepared slide underwent polyLIFT_h processing (488 nm laser wavelength). CBrCl₃ is activated by the laser light and oxidizes the substrate TM-THIQ to iminium ions according to liquid chromatography–mass spectrometry (Figure S18, Supporting Information). At the same time, the oxidized product is transferred to the acceptor slide, offering an efficient separation from the substrates. Based on the density functional theory (DFT) calculation, the iminium ions have a fully conjugated structure and narrower bandgap than TM-THIQ, resulting in the appearance of green fluorescence at around 536 nm only in iminium ions (Figure 4e). The acceptor slide is scanned at 532 nm and a strong fluorescence signal can be observed on both gradients and large areas (Figure S19, Supporting Information), while the control does not fluoresce, proving polyLIFT_h is capable of large-scale patterning. These results suggest that polyLIFT_h achieves in situ cross dehydrogenation coupling activation of TM-THIQ in milliseconds, offering a potentially rapid approach for high-throughput screening of photochemical reaction conditions and substrate scope.

2.5. Self-Healing of the Donor Film

Since laser irradiation causes permanent deformation of the polyimide donor during polyLIFT, the donor slide degrades quickly and hinders its reusability. Even if the polymer matrices can be self-healed, the absorber layer is gradually destroyed and the quality of a second transfer will be influenced. We transferred the whole area after self-healing (annealing at 95 °C for 1 h) of a previously used donor slide to show the stability and reusability of donors (Figure 5a). The area transfer from polyimide (Figure 5b) and hematite donor (Figure 5c) without self-healing treatment have obvious holes, which were generated by a pretransfer of a spot pattern. Comparing the transfer of a spot pattern from a polyimide and hematite donor under similar conditions, the resulting holes on the hematite donor

are about 50% smaller in diameter, while being around 3 times deeper (Figure 5d). Therefore, polyLIFT_h not only achieves a higher transfer resolution, but can also deliver more material per spot for femtoliter chemistry. For the area transfer from the donors with self-healing treatment, the holes on the polyimide layer still remain with smaller size (Figure 5e), suggesting the quality for a second transfer from the same donor is reduced by unhealable deformation. However, for hematite (Figure 5f), all holes disappear and a homogenous area transfer is achieved with the annealed and reused donor. Thus, the hematite donor can be reused after an annealing step, making it amenable to automation and transforming the method into a highly material-efficient technology.

3. Conclusion

We have developed a high-resolution LIFT process by introducing a new laser-absorber nanofilm. The film allows for efficient and highly precise delivery of materials and chemical reactions in femtoliter volumes. The hematite donor is synthesized in a facile annealing step of a Fe(NO₃)₃–PVA–PEG film that can be also applied for the generation of other transition metal oxide films. Hematite shows excellent wettability for both aqueous solutions and organic solvents. Precise spot arrays and homogenous area transfer of hydrophilic polymer matrices are obtained by polyLIFT_h, which is difficult for traditional polyimide donors. Different types of reactions were achievable in femtoliter polymer reactors with polyLIFT_h. For amide bond formation, a critical step in the synthesis of biomolecule microarrays, polyLIFT_h exhibits high densities of down to 30 μm pitch (>110 000 spots cm⁻²), which is comparable to expensive, scale- and speed-limited AFM-based scanning probe lithography technologies. Since also water-soluble polymers can be efficiently transferred from hematite donors (e.g., PVA), polyLIFT_h paves the way for many other chemical reactions by laser transfer, such as copper (I)-catalyzed azide-alkyne cycloaddition. More importantly, for the first time, we show an all-in-one transfer with in situ oxidation by laser irradiation, offering a potential way for high-throughput screening of reaction conditions and substrate scope in photochemistry. Finally, the polymer matrices on the hematite layer can be self-healed in an annealing step. These results have the potential to transform the LIFT process into a highly automated and material-efficient technology for diverse applications in high-throughput chemistry.

Supporting Information

Supporting Information is available from the Wiley Online Library or from the author.

Acknowledgements

This work was supported by the funding from the China Scholarship Council, the German Bundesministerium für Bildung und Forschung [BMBF, Grant No. 13XP5050A], the MPG-FhG cooperation [Glyco3Display], and the Max Planck Society. The authors would like to thank Jessica Brandt

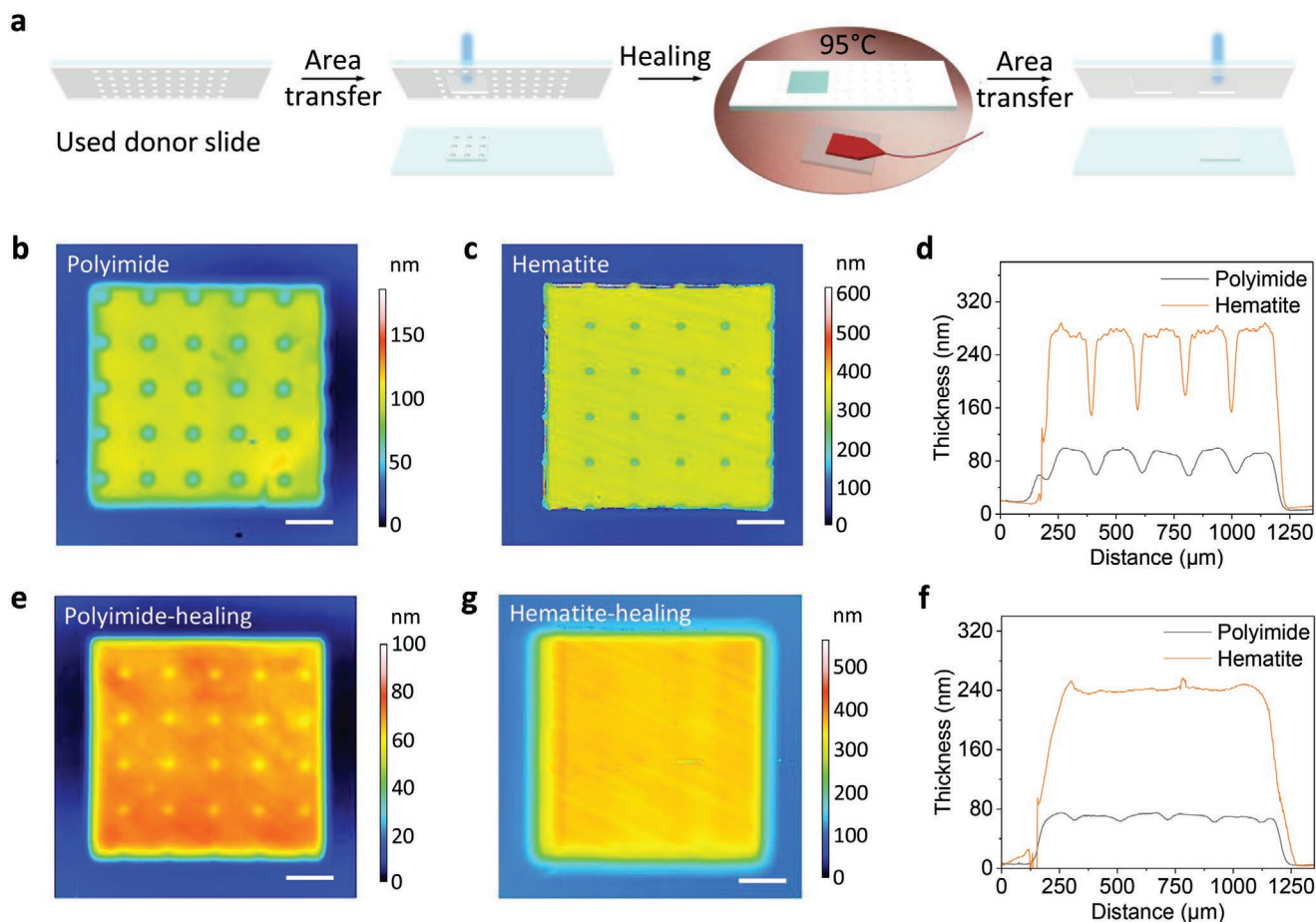


Figure 5. Self-healing of the polymer matrix film on donor slides. a) Process of self-healing: After the transfer of a spot pattern, the donor slide is annealed at 95 °C for 1 h in an oven. Afterward, a continuous area is transferred from the same location of the donor slide. b,e) Area transfer from polyimide donor without (b) and with (e) annealing step. c,g) Area transfer from hematite donor without (c) and with (g) healing step. d,f) Thickness profiles without (d) and with (f) annealing step. Scale bar: 200 μm .

for the ICP measurements and Prof. Chun-Ru Wang from the Chinese Academy of Sciences for support with XPS measurements.

Open access funding enabled and organized by Projekt DEAL.

Conflict of Interest

The authors declare no conflict of interest.

Data Availability Statement

The data that support the findings of this study are available from the corresponding author upon reasonable request.

Keywords

femtoliter chemistry, hematite films, laser-induced forward transfer, nanoabsorbers, solid phase synthesis

Received: October 22, 2021

Revised: December 7, 2021

Published online: January 17, 2022

- [1] a) E. K. Sackmann, A. L. Fulton, D. J. Beebe, *Nature* **2014**, *507*, 181; b) N. A. Dudukovic, E. J. Fong, H. B. Gameda, J. R. DeOtte, M. R. Cerón, B. D. Moran, J. T. Davis, S. E. Baker, E. B. Duoss, *Nature* **2021**, *595*, 58.
- [2] a) P. C. Chen, M. H. Liu, J. S. S. Du, B. Meckes, S. Z. Wang, H. X. Lin, V. P. Dravid, C. Wolverton, C. A. Mirkin, *Science* **2019**, *363*, 959; b) P. C. Chen, X. L. Liu, J. L. Hedrick, Z. Xie, S. Z. Wang, Q. Y. Lin, M. C. Hersam, V. P. Dravid, C. A. Mirkin, *Science* **2016**, *352*, 1565; c) X. Jia, J. Jiang, S. Zou, L. Han, H. Zhu, Q. Zhang, Y. Ma, P. Luo, P. Wu, A. Mayoral, X. Han, J. Cheng, S. Che, *Angew. Chem., Int. Ed.* **2021**, *60*, 14571.
- [3] N. Gupta, B. F. Lin, L. M. Campos, M. D. Dimitriou, S. T. Hikita, N. D. Treat, M. V. Tirrell, D. O. Clegg, E. J. Kramer, C. J. Hawker, *Nat. Chem.* **2010**, *2*, 138.
- [4] Y. Zhang, Y. Minagawa, H. Kizoe, K. Miyazaki, R. Iino, H. Ueno, K. V. Tabata, Y. Shimane, H. Noji, *Sci. Adv.* **2019**, *5*, eaav8185.
- [5] C. Carbonell, K. C. Stylianou, J. Hernando, E. Evangelio, S. A. Barnett, S. Nettikadan, I. Imaz, D. Maspoch, *Nat. Commun.* **2013**, *4*, 2173.
- [6] X. Liu, C. Carbonell, A. B. Braunschweig, *Chem. Soc. Rev.* **2016**, *45*, 6289.
- [7] R. Garcia, A. W. Knoll, E. Riedo, *Nat. Nanotechnol.* **2014**, *9*, 577.
- [8] S. T. Howell, A. Grushina, F. Holzner, J. Brugger, *Microsyst. Nanoeng.* **2020**, *6*, 21.

- [9] S. Eickelmann, A. Tsouka, J. Heidepriem, G. Paris, J. Zhang, V. Molinari, M. Mende, F. F. Loeffler, *Adv. Mater. Technol.* **2019**, *4*, 1900503.
- [10] U. Celano, *Electrical Atomic Force Microscopy for Nanoelectronics*, Springer, Cham, Switzerland **2019**.
- [11] a) A. Palla Papavlu, T. Mattle, S. Temmel, U. Lehmann, A. Hintennach, A. Grisel, A. Wokaun, T. Lippert, *Sci. Rep.* **2016**, *6*, 25144; b) S. Papazoglou, I. Zergioti, *Microelectron. Eng.* **2017**, *182*, 25.
- [12] F. F. Loeffler, T. C. Foertsch, R. Popov, D. S. Mattes, M. Schlageter, M. Sedlmayr, B. Ridder, F.-X. Dang, C. von Bojničić-Kninski, L. K. Weber, A. Fischer, J. Greifenstein, V. Bykovskaya, I. Buliev, F. R. Bischoff, L. Hahn, M. A. R. Meier, S. Bräse, A. K. Powell, T. S. Balaban, F. Breitling, A. Nesterov-Mueller, *Nat. Commun.* **2016**, *7*, 11844.
- [13] J. Zhang, Y. Zou, S. Eickelmann, C. Njel, T. Heil, S. Ronneberger, V. Strauss, P. H. Seeberger, A. Savateev, F. F. Loeffler, *Nat. Commun.* **2021**, *12*, 3224.
- [14] S. Eickelmann, S. Ronneberger, J. Zhang, G. Paris, F. F. Loeffler, *Adv. Mater. Interfaces* **2021**, *8*, 2001626.
- [15] M. Mende, A. Tsouka, J. Heidepriem, G. Paris, D. S. Mattes, S. Eickelmann, V. Bordoni, R. Wawrzinek, F. F. Fuchsberger, P. H. Seeberger, C. Rademacher, M. Delbianco, A. Mallagaray, F. F. Loeffler, *Chem. Eur. J.* **2020**, *26*, 9954.
- [16] G. Paris, A. Klinkusch, J. Heidepriem, A. Tsouka, J. Zhang, M. Mende, D. S. Mattes, D. Mager, H. Riegler, S. Eickelmann, F. F. Loeffler, *Appl. Surf. Sci.* **2020**, *508*, 144973.
- [17] L. E. Mathevula, L. L. Noto, B. M. Mothudi, M. Chithambo, M. S. Dhlamini, *J. Lumin.* **2017**, *192*, 879.
- [18] P. Sopeña, P. Serra, J. M. Fernández-Pradas, *Appl. Surf. Sci.* **2019**, *476*, 828.
- [19] B. Peng, A.-G. Thorsell, T. Karlberg, H. Schüler, S. Q. Yao, *Angew. Chem., Int. Ed.* **2017**, *56*, 248.
- [20] J. Atwater, D. S. Mattes, B. Streit, C. von Bojničić-Kninski, F. F. Loeffler, F. Breitling, H. Fuchs, M. Hirtz, *Adv. Mater.* **2018**, *30*, 1801632.
- [21] Y. Liu, P. H. Seeberger, N. Merbouh, F. F. Loeffler, *Chem. Eur. J.* **2021**, *27*, 16098.